



Lignocellulosic biomass degradation enzymes and characterization of cellulase and xylanase from *Bosea* sp. FBZP-16

Aicha Asma Houfani^{1,2,3} · Nico Anders² · Judith Loogen³ · Benedikt Heyman³ · Zahra Azzouz¹ · Azzeddine Bettache¹ · Jochen Büchs³ · Said Benallaoua¹

Received: 24 July 2021 / Revised: 19 October 2021 / Accepted: 20 October 2021
© The Author(s), under exclusive licence to Springer-Verlag GmbH Germany, part of Springer Nature 2021

Abstract

One key factor in the design of enzymatic cocktails for the lignocellulosic biomass breakdown is the performance of bacteria. *Bosea* sp. FBZP-16, a high-performing bacterium strain producing different types of cellulases and hemicellulases, was evaluated for production of global (hemi)cellulolytic enzymes under different growth conditions. Different (hemi)cellulases were predominantly produced. On Sigmacell 101 and newspaper, the highest specific cellobiohydrolase activity was found with 830.8 U/mg and 1341.2 U/mg, respectively. Beechwood xylan revealed the highest β -xylosidase activity (1625.3 U/mg) consistent with the highest xylose release. Cultivation temperature of 30 and 35 °C produced most (hemi)cellulolytic enzymes between the 3rd and the 9th days of incubation at shaking frequencies from 150 up to 300 rpm, while the highest glucose and xylose yields were observed at 150 rpm. Respiration activity monitoring system analysis confirmed the potential of *Bosea* sp. FBZP-16 to grow on xylan. The production of cellobiohydrolase and endoxylanase was further investigated using response surface methodology (RSM) and Box-Behnken matrix. The optimal conditions of the tested parameters were carbon source concentration (10 g/L), nitrogen source concentration (3 g/L), inoculum size (3 mL inoculum/100 mL media), and pH 7.0, where the maximal cellobiohydrolase production was found to be 2797 U/mg, which was close to the predicted activity of 2275.37 U/mg. The maximal endoxylanase production reached 60 U/mg, with a predicted value of 49.75 U/mg.

Keywords Cellulases · Hemicellulases · *Bosea* sp. FBZP-16 · Submerged fermentation · OFAT · RSM

Statement of Novelty This work is original and has not been published elsewhere or is currently being considered for publication. In this contribution, we address *Bosea* sp. FBZP-16 as an enzyme producer suitable for Biorefinery processes. In Biorefinery processes, *Bosea* sp. FBZP-16 can be used to produce substrate specific enzyme cocktails allowing for the hydrolysis of both cellulose and hemicellulose. The complete hydrolysis of cellulose and hemicellulose is crucial for Biorefinery processes to become economic. Thus, simultaneous on-site enzyme production for both natural polymers (cellulose and hemicellulose) is favorable to conventional enzyme purchasing an on-site optimization.

✉ Aicha Asma Houfani
a.a.houfani@gmail.com

¹ Laboratoire de Microbiologie Appliquée, Faculté des Sciences de la Nature et de la Vie, Université de Bejaia, 06000 Bejaia, Algeria

² Aachener Verfahrenstechnik-Enzyme Process Technology, RWTH Aachen University, Forckenbeckstraße 51, 52074 Aachen, Germany

³ Aachener Verfahrenstechnik-Biochemical Engineering, RWTH Aachen University, Forckenbeckstraße 51, 52074 Aachen, Germany

1 Introduction

Cellulose and hemicellulose derived from plant biomass, the most abundant polymers on Earth, are renewable resources obtained by carbon dioxide fixation via photosynthesis [46]. Access to the energy stored in these polymers is often achieved by simple combustion, which pollutes the environment. In contrast, the bioconversion using microbial enzymes enables to exploit the energy content of lignocellulosic biomass as alternative fuel source and, thereby, to reduce the dependence on fossil fuels.

Commercially available lignocellulose degrading enzymes mostly originate from fungi due to their high specific activity. Biomass-degrading enzymes from bacterial origin can supplement these existing fungal enzyme systems [12]. The corresponding conversion of lignocellulosic raw material to energy, fuel, and green chemical building blocks must be first developed and optimized on a small scale, starting with improving the enzymes for the conversion of lignocellulose to fermentable sugars. To this end, it is

crucial to understand the parameters influencing enzymatic biomass breakdown.

To study cell wall fractionation of lignocellulosic plant cells by microorganisms, the combined cellulase and hemicellulase production is relevant. The function of these enzymes is closely related [60]. Several studies focused on optimizing one individual enzyme involved in either cellulose or hemicellulose breakdown [13, 17]. Furthermore, improving enzymatic hydrolysis of both cellulose and hemicellulose using various substrates is an efficient strategy for the development of enzymatic cocktails [24]. Cellulose is degraded by the synergistic action of four enzymes (endoglucanase, exoglucanase, β -glucosidase, and lytic polysaccharide monooxygenase). Hemicellulose is mostly represented by xylan, which is mainly degraded by endo-1,4- β -xylanase and β -xylosidase acting on internal and terminal β -1,4 bonds in xylan, respectively. The internal cleavage by endo-1,4- β -xylanase releases shorter xylose oligomers and xylobiose. This last is cleaved by β -xylosidase into two separate D-xylose sugars [69].

Response surface methodology (RSM) has been widely used to determine optimal fermentation conditions in different areas of biotechnological interest including antimicrobial production [23, 53, 65, 66], drug delivery [10], antioxidant capacity [7, 11, 51], as well as enzymes activities [5, 6, 20, 26, 50, 67]. RSM combines individual, square, and interaction effects between variables [63]. The Box-Behnken design (BBD) was applied in the current study.

We report simultaneous production of cellobiohydrolase and endoxylanase using RSM in submerged fermentation (SmF). Many commercially produced microbial enzymes

are produced using SmF [64], which is particularly suitable for bacteria that require high humidity levels [47].

To determine (hemi)cellulosic enzymes activities, a broad range of methods and assays is used, including colorimetric, fluorometric assays, and chromatography-based methods [33]. The hydrolysis and degradation products need to be identified for a full characterization of biomass and a complete understanding of biomass degradation. Therefore, high-performance anion exchange chromatography with pulsed amperometric detection (HPAEC-PAD) is particularly suitable, since it may reveal a broad range of hydrolysis products.

The aim of this study was to exploit the diversity and specificity of bacterial enzymes involved in the degradation of (hemi)cellulose. Emphasizing variations in decomposition of cellulose and hemicellulose with different parameters, one-factor-at-a-time (OFAT) approach can assist us pinpoint particular catalytic features that are distinctive of *Bosea* sp. FBZP-16. This bacterium was screened on our previous genomic study in examining glycoside hydrolases (GH) among other isolated bacteria from the same environment. In fact, the genome of *Bosea* sp. FBZP-16 comprises 161 CAZymes, including 43 GH, 58 glycosyl transferases (GT), 4 polysaccharide lyases (PLs), 38 CEs, 15 AA, and 3 CBM, showing the strong potential of *Bosea* sp. FBZP-16 to degrade vegetable cell wall materials [35]. On the long term, the purification of various enzymes from the optimized cultivation conditions may facilitate the design of enzyme cocktails for the development of biorefineries using lignocellulosic biomass.

Table 1 Tested commercial cellulosic substrates and their characteristics

Cellulosic substrate	Solubility in water	Purity	<i>CrI</i> (%)	DP_w (AGU)	Particle size (μ m)	Supplier
α -cellulose	Insoluble ^b	Impure: xylane ^b	41.5 ^a	2140–2420 ^b	68.77 ^a	Sigma-Aldrich
Avicel PH101	Insoluble ^b	Pure ^b	82 ^b	200–240 ^b	~50 ^c	Fluka
CMC-4 M	Partially soluble ^c	99.5 ^c	-	~1000 ^c	-	Megazyme
Cellobiose	Soluble ^d	$\geq 98\%$ ^c	Amorphous	2	-	Carl Roth
Cellulose acetate	Insoluble ^d	$\geq 97.0\%$ ^c	-	-	-	Sigma-Aldrich
OrganoCat Cellulose	Insoluble ^d	-	0.4–0.7 ^d	400–1000 ^d	-	ITMC (RWTH Aachen University)
Sigmacell cellulose 20	Insoluble ^d	Pure ^d	52.6 ^a	-	20 ^c	Sigma-Aldrich
Sigmacell cellulose 50	Insoluble ^d	Pure ^d	56.1 ^a	-	50 ^c	Sigma-Aldrich
Sigmacell cellulose 101	Insoluble ^b	Pure ^b	Amorphous ^{a,b}	1590–1960 ^b	15.86 ^b	Sigma-Aldrich
Filter paper Whatman no. 1	Insoluble ^d	Pure ^d	~0.45 ^d	750–2800 ^d	-	GE Healthcare

CrI crystallinity index, DP_w polymerization degree estimated by molecular weight of the anhydroglucose unit (AGU)

^aAntonov et al. [4]

^bJäger et al. [37]

^cSupplier information

^dPercival Zhang et al. [57]; vom Stein et al. [70]; Grande et al. [30]

2 Material and methods

2.1 Carbon sources

Various simple and complex celluloses derived from lignocellulose with different physical properties were used as carbon source for cultivation (Table 1). The hemicellulosic carbon sources beechwood xylan, carob galactomannan, and wheat flour arabinoxylan were purchased from Megazyme (Wicklow, Ireland). In addition, pectin (Sigma-Aldrich, St. Louis, USA) and other mono- and disugar arabinose (Carl Roth GmbH, Karlsruhe, Germany), mannose (Carl Roth GmbH, Karlsruhe, Germany), galactose (AppliChem GmbH, Darmstadt, Germany), glucose (VWR International, Radnor, PA, USA), sucrose (Fluka, Buchs, Switzerland), and xylose (Biochem Chemopharma, France) were also tested as carbon sources. α -cellulose (Sigma-Aldrich, St. Louis, USA) and/or xylan from beechwood (Megazyme, Wicklow, Ireland) were also used for cellulolytic and hemicellulolytic activity determination, respectively. Furthermore, several complex biomasses were studied either with or without pretreatment. Physical pretreatment of lignocellulosic biomass by mechanical disintegration (milling, grinding, and sieving) and/or chemical pretreatments (Organosolv and lime) were performed prior to biological hydrolysis during cultivation

(Table 2). Composition of these carbon sources were previously described [34].

2.2 Organism and standard cultivation conditions

Bosea sp. FBZP-16 (GenBank KT868785) was obtained from the Laboratory of Applied Microbiology (University of Bejaia) collection.

Bosea sp. FBZP-16 preculture was used to inoculate 250-mL shake flasks with baffles with a filling volume of 40 mL standard medium, containing 5 g/L alpha-cellulose (Sigma-Aldrich) and 5 g/L beechwood xylan (Megazyme), 7 g/L KH_2PO_4 (Carl Roth), 2 g/L K_2HPO_4 (Carl Roth), 0.5 g/L $\text{MgSO}_4 \times 7\text{H}_2\text{O}$ (Carl Roth), 1 g/L $(\text{NH}_4)_2\text{SO}_4$ (Carl Roth), and 0.6 g/L yeast extract (Sigma-Aldrich), with pH adjusted to 7.0 [29]. Batch experiments were conducted in three independent biological replicates for 10 days at 30 °C and 200 rpm with a shaking diameter of 50 mm in a Kuhner shaker ISF1-X (Kühner AG, Birsfelden, Switzerland).

2.3 Analysis of bacterial growth on cellulose and hemicellulose

Bosea sp. growth on carbon sources was monitored by measuring the respiratory activity with an in-house constructed respiration activity monitoring system (RAMOS). The

Table 2 Pretreatment of tested lignocellulosic biomass

Type of biomass	Raw material	Pretreatment	Reference	
Cereal by-products	Barley awn	Drying at 105 °C for 24 h before and after Soxhlet extraction with 99.8% ethanol for 24 h	Anders et al. [3]	
	Barely straw			
	Oat flakes			
Peels	Wheat straw	Mechanical disruption using a screw press	Yan et al. [75]	
	Banana	Drying at 105 °C for 24 h before and after Soxhlet extraction with 99.8% ethanol for 24 h	Anders et al. [3]	
	Honeymelon			
	Lime			
Shells	Orange	Milling, sieving < 100 μm	Authors' laboratory collection	
	Watermelon			
	Coconut			
Woods	Peanut	Acid pretreatment: H_2SO_4 0,05 M, 170 °C/5 min	JRS J. Rettenmaier & Söhne GmbH + Co. KG, Rosenberg, Germany	
	Pistachio			
	Sawdust	Organosolv pretreatment: EtOH/Water 50/50 (v/v), 30 °C/30 min, 160 °C/30 min, 160 °C/5 h		
	Beechwood			
Miscellaneous biomass	Spruce wood	Lime pretreatment: $\text{CaCO}_3 \sim 0,09$ M, 6 °C/min, 120 °C/60 min	Anders et al. [3]	
	Lawn grass	Drying at 105 °C for 24 h before and after Soxhlet extraction with 99.8% ethanol for 24 h		
	Newspaper	Paper discs ~ 3 mm using a hole-punch (Leitz, Germany)		Medouni-Haroune et al. [52]
	Olive pomace	Drying at room temperature, 3 weeks \leq 1 mm		
	<i>Silphium perfoliatum</i>	Milling, sieving \leq 1 mm	Lunze et al. [48]	

RAMOS system monitors the metabolic activity of aerobic microorganisms. The system is equipped with sensors for measuring the oxygen transfer rate (OTR) and the carbon dioxide transfer rate (CTR). The OTR describes the transfer of oxygen from the gas phase into the medium, whereby the $k_L a$ value (volumetric mass transfer coefficient) can be regarded as a measure of efficiency. The DOT (dissolved oxygen concentration) describes the dissolved oxygen tension in the medium. The uptake of dissolved oxygen by the microorganism is described by the OUR (oxygen uptake rate). In an aerobic cultivation, it is assumed that the OTR is very close to the OUR. Since the OTR is measured or calculated, the oxygen uptake of the microorganisms over the cultivation time is known. The OTR can be calculated with the following formula:

$$\text{OTR} = k_L a (C^* - C_L)$$

$$\text{OTR} = [\text{mgO}_2/\text{L}/\text{h}]$$

k_L	oxygen transfer coefficient (cm/h).
a	gas–liquid interfacial area per unit vol. (cm^2/cm^3).
$k_L a$	volumetric oxygen transfer coefficient (1/h).
C^*	saturated oxygen concentration (mg/L).
C_L	oxygen concentration in the broth (mg/L).

The $k_L a$ value is a key figure for the transport of oxygen from the gaseous phase to the medium of a RAMOS flask. It is assumed that the transport of oxygen through the gas/liquid interface is the rate-determining step. The following relationship applies: $dC/dt = k_L a \cdot (C^* - C_L)$, where C_L is the dissolved gas concentration and C^* is the equilibrium concentration at the phase interface or, in other words, the maximum solubility [1, 2].

For determination of growth in the presence of cellulose and hemicellulose, the cultivation was carried out in the presence of 10 g/L α -cellulose and 10 g/L beechwood xylan, respectively. Eight parallel RAMOS 250-mL shake flasks were used with a filling volume of 30 mL and a shaking frequency of 250 rpm, with all other conditions as outlined above (Section 2.2). The culture was performed in duplicates.

2.4 Variation of cultivation conditions for enzyme production

The cultivation conditions were studied by the OFAT approach. The effect of carbon and nitrogen sources, temperature, incubation time, and agitation was varied by maintaining all factors constant, as outlined above, using the standard cultivation conditions except the one being studied. All cultivation experiments were performed in triplicates.

- The effect of the listed carbon and energy sources were studied at a concentration of 10 g/L instead of cellulose/beechwood xylan (Table 1).
- The effect of organic (malt extract, tryptone-peptone-casein, and yeast extract) and inorganic nitrogen sources (KNO_3 , NaNO_3 , NH_4NO_3 , and $(\text{NH}_4)_2\text{SO}_4$) was investigated at a concentration of 2 g/L.
- To determine the optimum temperature, the strain was cultivated at temperatures ranging from 25 to 40 °C.
- The effect of incubation period was studied by carrying a fermentation experiment for up to 10 days, where the enzyme production was measured at 24 h intervals.
- To study the effect of agitation, cultivations were performed at shaking frequencies ranging from 0 to 300 rpm.

2.4.1 RSM

Experiment-based optimization using the BBD is performed with 27 experiments designed in Design Expert 10 (Stat-Ease, Minneapolis, MN) to determine the optimum of four culture medium parameters (Table 3). The following parameters were studied: carbon source concentration (1, 10, 19 (g/L)), nitrogen source concentration (1, 2, 3 (g/L)), pH (6.5, 7, and 7.5), and inoculum size (i.e., inoculum volume: 1%, 2%, and 3% (v/v)). The four parameters were chosen in such a way to reduce experimental efforts and as strongly affecting parameters in (hemi)cellulase production. Design Expert 10 (Stat-Ease, Minneapolis, MN) software was used for graphical analysis of interaction effects between tested parameters and statistical analysis.

2.5 Enzyme assays

Endo-1,4- β -glucanase and endo-1,4- β -xylanase activities produced in liquid or submerged culture were assayed using liquid Azo-CMC 2% w/v and Azo-Xylan 1% w/v substrates (Megazyme, Ireland), respectively, following supplier's instructions with some modifications as previously described [8], and determined by referring to a standard curve. Crude supernatant (0.15 mL) to be tested was added to 0.15 mL of azo-substrate reagent and mixed by vortexing. The mixture was incubated at 40 °C for 30 min in a microbiological incubator (Binder, Germany). The reaction was stopped by the addition of 750 μL of absolute ethanol for endoglucanase and endoxylanase assays, respectively. The reaction was vortexed and centrifuged at 14,000 g for 10 min. The absorbance of the crude supernatant was determined at 595 nm in sterile cell culture microplates reference 677102 (Greiner Bio-One GmbH, Germany). In a Synergy 4 Microplate Reader (BioTek, Winooski, VT, USA) using distilled water as blank in triplicate. Based on standard curves correlating dye release with reducing sugar release, enzyme

Table 3 Experimental matrix by coding unit and obtained actual values of the Box-Behnken design

Run	Carbon source concentration (A)	Nitrogen source concentration (B)	Inoculum size (C)	pH (D)	Cellobiohydrolase (U/mg)	Endoxy-lanase (U/mg)
1	0	0	-1	-1	2.49	21.14
2	0	0	1	-1	3.70	5.85
3	0	0	-1	1	42.13	27.77
4	0	0	1	1	3.15	30.71
5	-1	-1	0	0	1328.01	38.02
6	-1	1	0	0	1117.56	18.42
7	1	-1	0	0	37.81	26.86
8	1	1	0	0	31.95	2.32
9	0	-1	0	-1	23.81	26.35
10	0	1	0	-1	73.25	19.03
11	0	-1	0	1	18.55	22.73
12	0	1	0	1	18.26	10.22
13	-1	0	-1	0	51.62	4.10
14	1	0	-1	0	433.25	12.75
15	-1	0	1	0	233.91	2.15
16	1	0	1	0	587.49	30.14
17	-1	0	0	-1	348.42	54.30
18	1	0	0	-1	333.17	4.13
19	-1	0	0	1	64.76	6.45
20	1	0	0	1	113.86	31.02
21	0	-1	-1	0	607.66	60.00
22	0	1	-1	0	532.55	4.45
23	0	-1	1	0	360.36	11.98
24	0	1	1	0	2796.59	7.56
25	0	0	0	0	35.18	5.89
26	0	0	0	0	71.51	12.71
27	0	0	0	0	4.93	57.45

High level (+1), medium level (0), low level (-1)

activity was calculated, where one unit of enzyme activity corresponded to 1 nmol of reducing sugar released per minute by the enzyme.

Measurement of cellulase activities (cellobiohydrolase and β -glucosidase) and xylanase activities (β -xylosidase, β -mannosidase, β -galactosidase, arabinosidase, α -glucuronidase, and α -glucosidase) was performed with 4-methylumbelliferone (MUF)-linked substrates (Glycosynth, UK). Enzymatic assays were performed in triplicate on a flat-bottomed non-binding 96-well microplate with flat bottom, black color with transparent bottom reference 655087 (Kisker Biotech, Germany). The test was performed with 200 μ L of substrate (2.50–2.75 mM, solubilized in DMSO) and 40 μ L of enzymatic extract [8]. The reaction mixtures were incubated at 40 °C in the dark in a microbiological incubator (Binder, Germany). Fluorescence was read using the Infinite Microplate Reader (TECAN, Austria) after 5 min and 125 min at 355 nm excitation and 460 nm emission. The enzymatic activities were determined on a

standard curve of MUF and expressed in nanomoles per minute per milliliter.

The protein concentration in the culture crude supernatant was determined using the Pierce BCA Protein Assay Kit (Thermo Fisher Scientific, USA) and was performed according to the supplier instructions for microtiter plates. Bovine serum albumin (BSA) in a concentration range between 25 and 2000 μ g/mL was used for the standard curve. The absorption after the assay reaction of the calibration standards and the enzyme solutions after incubation at 37 °C for 30 min was measured at 562 nm in a 96-well microtiter plate (MTP) using the Synergy 4 Microplate Reader (BioTek, USA) with Gen5 2 Data Analyses software. The specific enzymatic activity was calculated by referring the volumetric enzymatic activity results to the protein concentration.

Two-way ANOVA and Tukey's test were used for multiple comparison between the enzymatic activities obtained under various conditions. Differences were considered significant when the p -values < 0.05.

2.6 Photometric sugar analysis

The para-hydroxybenzoic acid hydrazide (PAHBAH) assay was used for quantifying the total amount of reducing sugars (glucose and xylose) released in the fermentation broth [45]. For PAHBAH reagent A, 5 g 4-hydroxybenzoic acid hydrazide, 30 mL H₂O (dist.), and 5 mL HCl (37%) are mixed and filled up to 100 mL with H₂O (dist.). For reagent B, 12.5 g trisodium citrate, 1.1 g CaCl₂, and 20 g NaOH are dissolved in 500 mL H₂O (dist.) and filled up to 1 L with H₂O (dist.). The PAHBAH working solution was prepared immediately before performing the assay by mixing one part of reagent A and ten parts of reagent B. Samples (75 µL) were mixed with 150 µL working reagent in a 2-mL tube and incubated for 10 min at 900 rpm and 100 °C on a thermo mixer (MHR23, HLC Biotech, Germany). After cooling to room temperature, samples were transferred to a flat-bottom MTP (9293.1, Roth, Germany), and absorbance was measured at 410 nm (Synergy 4 Microplate Reader, BioTek, USA). Product concentrations were calculated from a calibration with glucose and xylose with a concentration of 0–0.5 g/L.

2.7 SDS-PAGE

Polyacrylamide gel electrophoresis treated with sodium dodecyl sulfate (SDS-PAGE) was applied to the cultivation crude supernatants obtained by centrifuging the fermentation broth at 4000 rpm, 4 °C for 20 min. NuPAGE Novex 12% Bis–Tris Mini Gel gels (Invitrogen, USA) and samples were prepared according to the manufacturer's protocol and the method described previously [36]. Proteins were stained with Roti®-Blue 5× concentrate molecular weight marker (Carl Roth, Germany). Electrophoresis was performed according to the manufacturer's protocol (Invitrogen, USA). The gels were scanned using the Perfection V700 scanner (Epson, Japan).

2.8 Chromatographic sugar analysis (HPAEC-PAD)

An adapted online automatic method using high-performance anion exchange chromatography with pulsed amperometric detection (HPAEC-PAD) was used for simultaneous determination of mono- and oligosaccharides resulting from both cellulose (glucose, cellobiose, cellotriose, and 5-hydroxymethylfurfural (5-HMF) and hemicellulose (arabinose, galactose, mannose, rhamnose, xylose, xylobiose, and xylotriose) decomposition released in the fermentation broth. HPAEC-PAD analysis of cellulose and hemicellulose degradation products is generally performed as described by Anders et al. [3] and Cürten et al. [21]. The HPAEC-PAD system was an ICS-5000+ system purchased from Thermo

Scientific equipped with an AS-AP autosampler as described in [39–41]. The flow was 1.0 mL/min of 100 mMol sodium hydroxide with a column temperature of 30 °C. The injection volume was 5 µL. The software used for measurement and data calculation was Chromeleon with a calibration range according to Anders et al. [3]. Average retention time for all measurement was 3.415 min.

3 Result

3.1 Characterization of (hemi)cellulases under various cultivation conditions

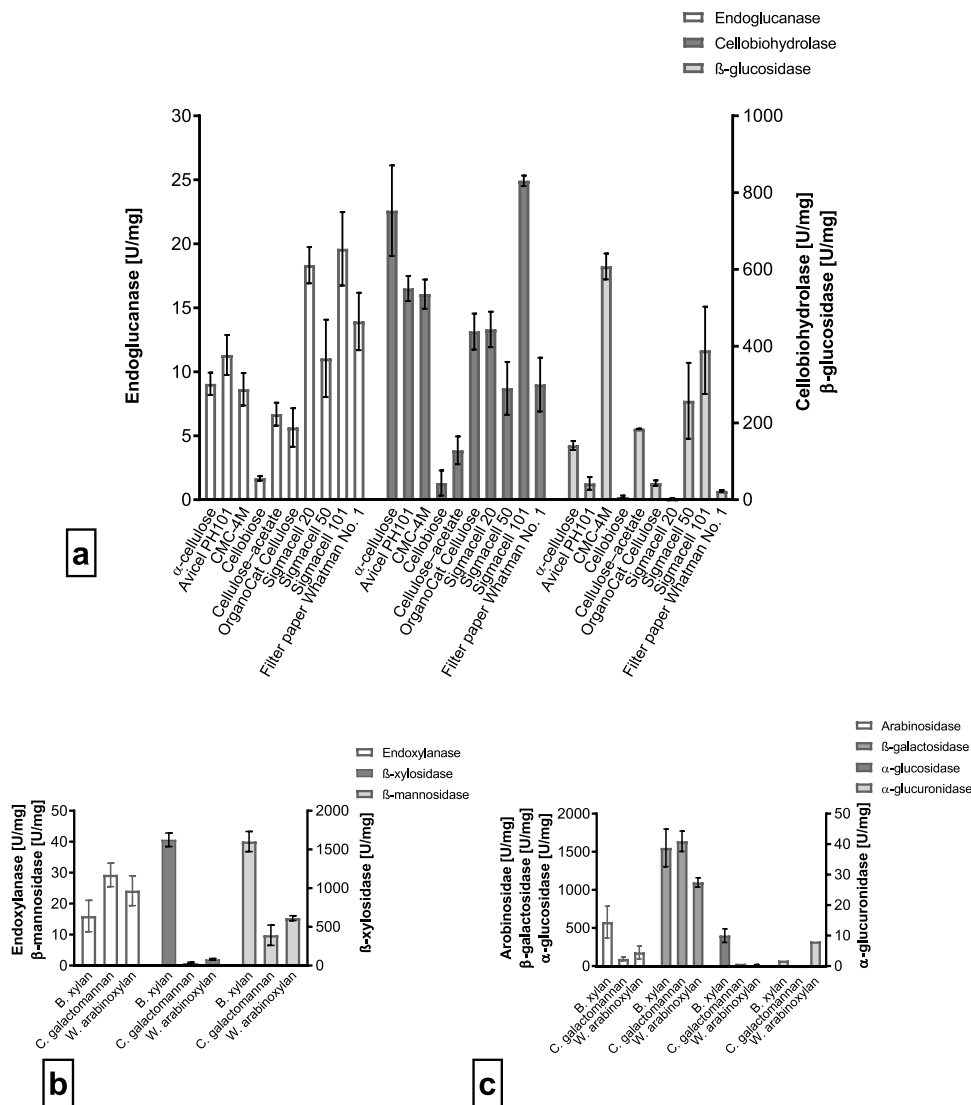
No significant difference in endoglucanase activity between the tested cellulosic substrates was determined by using the Tukey's multiple comparison test (Fig. 1a). However, cellobiohydrolase activity was significantly the highest on newspaper (Table 4). CMC-4 M enabled the highest β-glucosidase production. PAHBAH assay showed higher glucose release on cellobiose, followed by CMC-4 M (Fig. S-1a). With HPAEC-PAD analysis, the hydrolysis products of the tested substrates showed that glucose was the main component of sugar products, with a concentration to a maximum of 54.5 mg/L on CMC-4 M, followed by a concentration of 42.1 mg/L on cellobiose.

There was no significant difference in endoxylanase, β-mannosidase, and α-glucuronidase activities between the tested hemicellulosic substrates (Fig. 1b, c). However, beechwood xylan revealed the best activities of β-xylosidases, arabinosidases, and α-glucosidases. Apart from that, β-galactosidases were higher with carob galactomannan followed by beechwood xylan, but without a significant difference. Both preliminary PAHBAH test (1120.5 mg/L) and HPAEC-PAD (21.3 mg/L) showed the highest xylose release on beechwood xylan.

The culture crude supernatant showed that there were no significant differences in endoglucanase activities. The highest cellobiohydrolase activities were observed with newspaper, while those from β-glucosidase on olive pomace and pistachio shell (Fig. S-2). There was no significant difference between the activities of endoxylanase and α-glucuronidase among the tested lignocellulosic substrates (Fig. S-3). Sawdust showed maximum activities of β-xylosidase, β-mannosidase, and α-glucosidase. The activities of arabinosidase and β-galactosidase were higher with banana peels and oat flakes.

The PAHBAH test revealed a higher glucose level with oat flakes (617.2 mg/L), followed by grass (505.2 mg/L) while HPAEC-PAD analysis indicated a higher glucose yield with pistachio shell (91.0 mg/L) and xylose yield with sawdust (31.0 mg/L) (Fig. 2).

Fig. 1 Effect of different (hemi)cellulosic carbon sources on cellulases (**a**), depolymerization hemicellulases (**b**), and accessory hemicellulases (**c**)



When other simple carbon sources were used (Fig. S-4), endoglucanases were higher in the presence of galactose. Cellobiohydrolase activities were maximal in the presence of xylose. Mannose induced β -xylosidases and β -mannosidases. β -glucosidases were also higher with mannose compared to glucose, arabinose, galactose, and xylose. Sucrose induced arabinosidases and β -galactosidases. Endoxylanases were also higher in the presence of sucrose with a significant difference only with respect to arabinose. There was no significant difference between the other carbon sources tested to produce α -glucosidases and α -glucuronidases.

The separation of cultures grown on cellulosic and hemicellulosic substrates gave molecular masses ranging around 28 to 78 kDa (Fig. S-5). The analysis of Sigmacell cellulose type 20 revealed three bands with molecular masses of about 28, 41, and 70 kDa, while no bands were detected in Sigmacell cellulose type 50 and 101 (Fig. S-5a.). The 70-kDa protein was also detected on cellobiose and OrganoCat

cellulose. A similar band of about 60 kDa appeared both on Avicel and CMC. Furthermore, Avicel had an additional band of about 50 kDa. The other cellulosic substrates α -cellulose, cellulose acetate, and filter paper Whatman no. 1 do not show any protein formation in the SDS-PAGE. On beechwood xylan, four protein bands of about 33, 41, 44, and 60 kDa were detected. This latter was also detected on wheat arabinoxylan in addition to the highest molecular weight protein band of about 78 kDa. Carob galactomannan showed a single protein band of about 56 kDa. The protein bands of ~ 41 and 60 kDa were detected on both cellulosic (Sigmacell cellulose 20, Avicel, CMC) and hemicellulosic substrates (beechwood xylan, wheat flour arabinoxylan).

There was no significant difference between the tested nitrogen sources for the activity of endoglucanases and β -glucosidases (Fig. S-6). However, better cellobiohydrolase activities and high glucose yields (PAHBAH test) were observed with malt extract. The maximum production of

Table 4 Best carbon and nitrogen sources for obtaining enzyme activity

Enzyme	Optimized condition					
	Carbon sources			Nitrogen sources		
	Best	Specific enzyme activity (U/mg)	<i>p</i> value	Best	Specific enzyme activity (U/mg)	<i>p</i> value
Cellulases						
Endoglucanases	Galactose	329.6	=0.0023 vs xylose <0.0001 vs others	NaNO ₃	20.4	ns
Cellobiohydrolases	Newspaper	1341.2	<0.0001	Malt extract	889.3	<0.0001
β-glucosidases	CMC-4 M	607.7	<0.0001	Yeast extract	203.8	
Hemicellulases						
Endoxylanases	Newspaper	105.7	ns	Yeast extract	39.8	ns
β-xylosidases	Newspaper	1625.3	<0.0001 vs B. xylan and sawdust =0.0012 vs Pistachio ns vs others	(NH ₄) ₂ SO ₄	110.5	<0.0001
β-mannosidases	Sawdust	386.4	ns vs olive pomace 0.0361 vs lime peel 0.001 vs wheat straw 0.0008 vs mannose 0.0005 vs Barely awn 0.0003 vs Banana peel 0.0001 vs Barely straw, <i>S. perfoliatum</i> and sucrose <0.0001 vs others	KNO ₃	33.2	ns vs malt extract and (NH ₄) ₂ SO ₄ 0.0127 vs NH ₄ NO ₃ 0.01 vs tryptone-peptone-casein 0.0095 vs NaNO ₃ 0.0015 vs yeast extract
Arabinosidases	Sucrose	1360.2	ns vs banana peel <0.0001 vs others	Yeast extract	131.8	ns
β-galactosidases	Oat flakes	2290.0	<i>p</i> =0.0032 vs sucrose <0.0001 vs others	Yeast extract	690.4	<0.0001
α-glucosidases	Wheat straw	1140.4	<0.0001	Yeast extract	37.4	ns
α-glucuronidases	Mannose	73.6	ns	Malt extract	2.04	ns

ns not significant

endoxyanases was obtained with yeast extract. The yeast extract also induced a better production of β-galactosidases. The production of β-xylosidases was optimal with (NH₄)₂SO₄ as a nitrogen source. No significant difference was observed in the production of arabinosidases, α-glucosidases, and α-glucuronidases. The β-mannosidases were higher in the presence of KNO₃. However, no significant difference was observed with malt extract and (NH₄)₂SO₄. Using KNO₃, the highest yield of xylose with PAHBAH-analysis was determined. HPAEC-PAD analysis showed a higher glucose yield with tryptone-peptone-casein (3.66 mg/L).

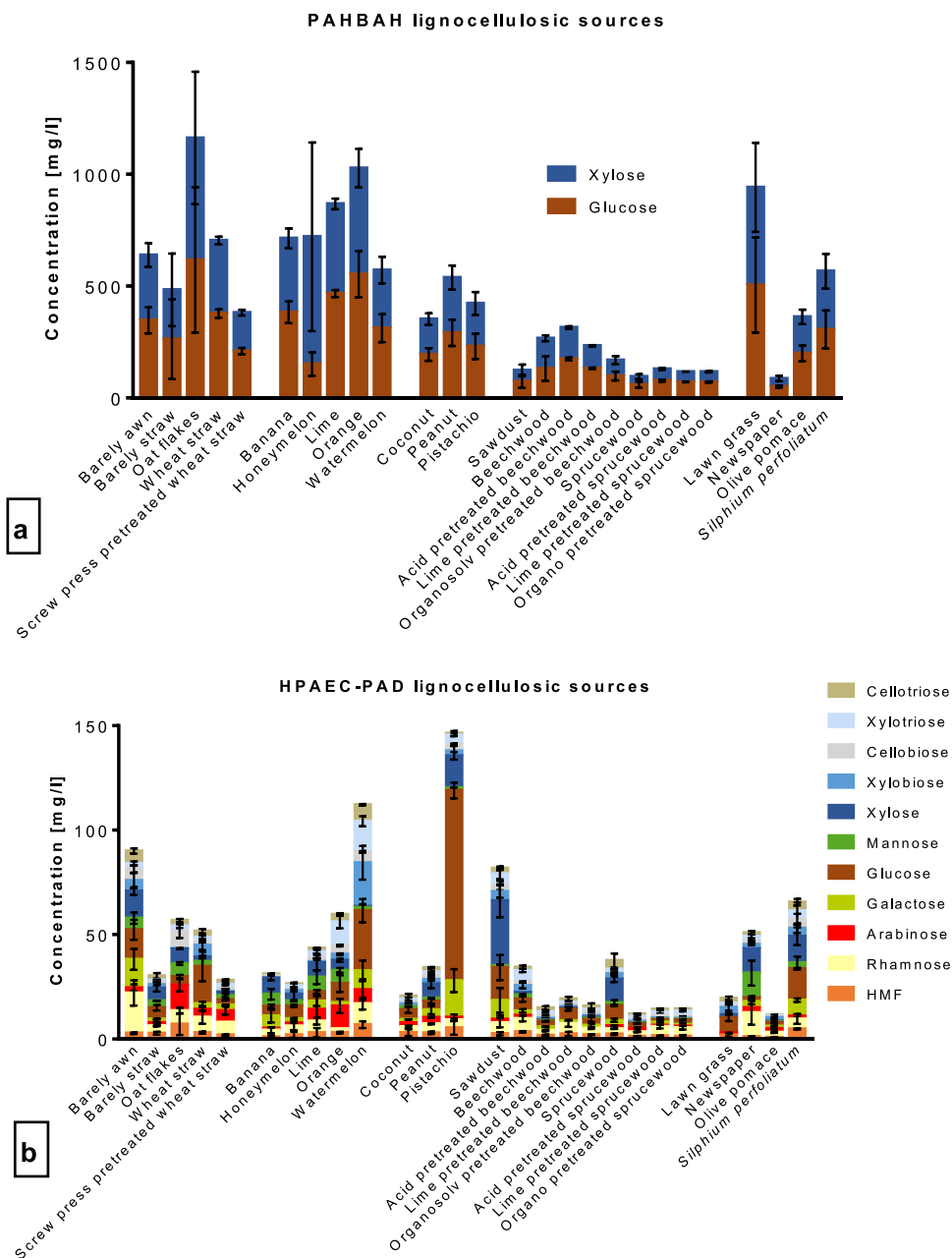
The optimal temperature for endoglucanase, endoxylanase, and β-xylosidase production was 30 °C (Fig. S-7). PAHBAH assay revealed higher glucose and xylose release at 30 °C. β-glucosidase was quite similarly produced from 25 to 35 °C and decreased at 40 °C. Extremely low activity of α-glucuronidase was only produced at 30 °C. At 35 °C, there was better production of cellobiohydrolase, β-mannosidase, arabinosidase, β-galactosidase, and α-glucosidase.

HPAEC-PAD analysis revealed higher xylose, xylobiose, and cellobiose yield at 30 °C. A decline in enzyme production beyond 35 °C was also observed. However, glucose and 5-HMF were higher at 40 °C. Most of the enzymes were produced at 30 °C or 35 °C, whereas enzyme production decreased at 40 °C.

The optimal shaking frequency for endoglucanase and cellobiohydrolase occurred at 200 rpm (Fig. S-8). Extremely low activity of α-glucuronidase was only produced at 200 rpm. The highest β-glucosidase was produced at 250 rpm. The highest activities of endoxylanase, β-xylosidase, β-galactosidase, and α-glucosidase were produced at 150 rpm. Both PAHBAH and HPAEC-PAD analyses showed higher glucose and xylose yield at 150 rpm. At 300 rpm, there was better recovery of β-mannosidase and α-glucosidase.

The maximum production of β-xylosidases (87.28 U/mg), arabinosidases (86.35 U/mg), β-galactosidases (582.80 U/mg), and α-glucuronidases (42.14 U/mg) was reached at the 5th day of incubation (Fig. S-9). The

Fig. 2 Different lignocellulosic carbon sources effect on hydrolysis products with PAHBAH test (a) and HPAEC-PAD (b)



optimal activities of endoglucanases (40.04 U/mg) and endoxylanases (30.36 U/mg) were observed at day 6, that of β -glucosidases (348.7 U/mg) at day 7, and cellobiohydrolases on the 9th day of incubation. β -mannosidases were produced only during the first 3 days, and no α -glucosidase activity was detected.

3.2 Response surface methodology

The RSM experiments using BDD were conducted to determine the optimal values and effect of four variables *A* (carbon source concentration), *B* (nitrogen source concentration), *C* (inoculum size), and *D* (pH). The results of

experimental cellobiohydrolase and endoxylanase production experiments of the BDD are shown in Table 3. The *p*-values were used to identify the effect of each factor on enzymatic production. The optimization of both cellobiohydrolase and endoxylanase-specific activities indicated that the model was significant ($p < 0.05$), with no significant lack of fit. The best pH value for optimal releasing of cellulases lies in 7.0.

RSM was performed to show the interaction between variables that significantly affect enzyme production. The interactions *CD*, *C*², and *D*² were statistically significant for cellobiohydrolase production (Table 5), while endoxylanase

Table 5 ANOVA of the Box-Behnken design

Enzyme	Cellulohydrolase			Endoxylanase		
	ANOVA for quadratic model	Mean square	F-value	p-value	Mean square	F-value
Model	5.67E+05	5.03	0.004	462.67	6.18	0.0016
A—carbon source concentration	2.54E+05	2.26	0.159	2317.56	30.94	0.0001
B—nitrogen source concentration	8938.19	0.0793	0.783	3.32	0.0443	0.8368
C—inoculum size	1.03E+06	9.17	0.0105	43.17	0.5762	0.4624
D—pH	7.36E+05	6.53	0.0252	65.21	0.8705	0.3692
AB	1.23E+05	1.09	0.3164	220.81	2.95	0.1117
AC	4.22E+05	3.75	0.0768	149.68	2.00	0.1829
AD	85,728.32	0.7609	0.4002	399.49	5.33	0.0395
BC	1.09E+05	0.9696	0.3442	43.34	0.5786	0.4616
BD	22,205.96	0.1971	0.665	36.23	0.4836	0.5000
CD	3.61E+06	32	0.0001	59.55	0.795	0.3901
A ²	28,994.77	0.2573	0.6211	2279.69	30.43	0.0001
B ²	51,115.93	0.4537	0.5134	106.33	1.42	0.2565
C ²	6.03E+05	5.35	0.0392	677.47	9.04	0.0109
D ²	5.49E+05	4.87	0.0475	39.03	0.5211	0.4842
Lack of fit	1.29E+05	4.07	0.2134	86.47	5.05	0.1765
Fit statistics						
Adjusted R ²		0.6845			0.736	
Adeq. precision		10.4438			8.985	

production was significant with the interactions *AD*, *A*², and *B*².

In the studied matrix, maximum and minimum cellulohydrolase productions of 2796.56 U/mg and 2.49 U/mg were obtained in run 24 (pH = 7, inoculum size = 3%, carbon source concentration = 10 g/L, and nitrogen source concentration = 3 g/L) and run 1 (pH = 6.5, inoculum size = 1%, carbon source concentration = 10 g/L, and nitrogen source concentration = 2 g/L), respectively. Maximum endoxylanase production was of 57.45 U/mg in run 27 (pH = 7, inoculum size = 2%, carbon source concentration = 10 g/L, and nitrogen source concentration = 2 g/L) and minimal production of 2.15 U/mg in run 15 (pH = 7, inoculum size = 3%, carbon source concentration = 1 g/L, and nitrogen source concentration = 2 g/L). Interaction effects between *A*, *B*, *C*, and *D* were identified by 2D and 3D response surfaces of the quadratic model in Fig. 3. Perturbation plots are shown in Fig. 4. The correlation between predicted values and actual values is represented in Fig. 5.

For cellulohydrolase, the coefficient of determination (*R*²) was found with a predicted *R*² = 0.8544 and an adjusted *R*² = 0.6845, while for endoxylanase production, predicted *R*² = 0.8781 and adjusted *R*² = 0.736. The values of adequate precision (Adeq precision) measured were 10.4438 and 8.985, respectively.

3.3 Cultivations carried out in the RAMOS device

Respiration activity monitoring of the bacterium *Bosea* sp. FBZP-16 was performed in RAMOS device for the measurement of OTR, using beechwood xylan and α -cellulose as main carbon sources in the presence of minerals and yeast extract. *Bosea* sp. FBPZ-16 was confirmed as xylan degrader, since a significant OTR was observed (Fig. S-13a). The OTR increased to a maximum of ~8 mmol/L/h and then started decreasing slowing after 2–3 days of cultivation. Xylan degradation occurred in two phases, as shown by the double peaks. However, the cellulolytic enzymes of *Bosea* sp. FBZP-16 were not able to degrade cellulose. No significant OTR was detected when α -cellulose was used as carbon source (Fig. S-13b).

SDS-PAGE (Fig. S-5) showed that there were five protein bands of about 28, 42, 50, 54, and 70 kDa in RAMOS samples when cellulose and xylan in presence of glucose were used as carbon sources.

4 Discussion

Bosea sp. FBZP-16 has been previously shown to degrade (hemi)cellulose using a combination of enzymatic assays and genomic approach [35]. Here, the strain was biochemically characterized to determine further insights on the plant biomass degradation capabilities. Varying carbon sources and operating conditions (pH, temperature, shaking frequency)

were analyzed for potential impact on the released enzymes and sugars in the fermentation supernatant broth.

For an efficient lignocellulosic biomass conversion from *Bosea* sp. FBZP-16, the optimal operation conditions were studied to simplify the scale-up to future production scale and to determine its potential in purification, by using different lignocellulosic and commercial substrates. Both the enzyme activities and the hydrolysis products were investigated in culture crude supernatants of *Bosea* sp. FBZP-16 by varying medium composition with respect to carbon and nitrogen sources, temperature, shaking frequency, and incubation period. First, various (hemi)cellulosic carbon sources were tested for their effect on (hemi)cellulolytic activities and released hydrolysis products.

Overall, the degradation and enzyme activities on hemicellulosic substrates were higher in terms of enzyme activities. Beechwood xylan was the best substrate to produce different hemicellulolytic enzymes. This could be due to its unbranched structure compared to branched galactomannan and arabinoxylan [71]. Improved xylanase activity has also been reported in a strain of *Flavobacterium* sp. in the presence of beechwood xylan in comparison with wheat and rye arabinoxylan [44]. Furthermore, beechwood xylan is more amorphous than wheat flour arabinoxylan [25]. In a similar conducted study on bacterial xylanases, the bacterial strain *Bacillus safensis* CBLMA18 revealed a xylanase with the highest specific activity on beechwood xylan in comparison to other xylanolytic substrates (oat spelt xylan, wheat arabinoxylan, rye arabinoxylan, and 4-*o*-methyl glucuronoxylan) [18].

Although xylanase activities are often higher than cellulase activities, the release of fermentable sugars is more important following cellulose decomposition. This may be probably due to cellulose and hemicellulose structures. Indeed, cellulose is a homopolymer, which contains only glucose, while hemicellulose is a heteropolymer composed of a mixture of sugars [49].

The values obtained with the preliminary PAHBAH test were always higher than by chromatographic methods. This massive deviation can be explained by the non-distinction of PAHBAH test in comparison with HPAEC-PAD for the different monomeric and oligomeric sugars [21]. Thus, hydrolysis products were analyzed for detailed information on monomeric and oligomeric concentration using the HPAEC-PAD. Additionally, sugar degradation products can interfere and change the correct sugar values.

Different types of lignocellulosic substrates were tested including forestry (wood), agricultural (cereals) and domestic residues (fruits peeling). These resources differ in the content of cellulose and hemicellulose as reported previously [33]. Surprisingly, many enzymes were highly produced on milled woody materials, such as sawdust, which indicates a good penetration of these enzymes on lignified

substrates. Several hemicellulolytic activities were higher on sawdust as lignocellulosic natural carbon source. The bacterium *Arthrobacter* sp. MTCC6915 also displayed xylanase activity in sawdust under solid state fermentation [54]. The differences of the carbon source used, i.e., complex lignocellulosic vs. pure (hemi)cellulosic substrates and the degree of crystallinity of the different available commercial (hemi)cellulosic substrates, play a major role in enzyme activity. Indeed, higher cellulases activities and glucose yield were observed on amorphous cellulose, in this case: Sigmacell cellulose 101 and CMC-4 M [74]. The later has approximately 4 carboxymethyl groups per 10 anhydroglucose units, resulting in high water solubility that facilitates its degradation.

Bosea sp. FBZP-16 was shown to be able to use different carbon compounds as substrates for growth that were confirmed by bands detection when running electrophoretic SDS-PAGE. The presence of certain bands on both cellulosic and hemicellulosic substrates might be explained by the presence of a bifunctional cellulase-xylanase activity [68]. At the genetic level, endo-1,4- β -glucanases in *Bosea* sp. FBZP-16 were affiliated to glycoside hydrolase families GH5 and GH8 and hemicellulolytic deconstructing genes in families GH2 and G120 [35]. Different glycosidic bonds (β -1-4, β -1-6, etc.) are cleaved by endoglucanases for different substrates. Known as endo-1,4- β -glucanases (1,4- β -D-glucan glucanohydrolase, EC 3.2.1.4), these enzymes more commonly cleave β -1-4-glycosidic bonds [59]. The 41-kDa band protein was similarly reported on *Lysobacter* sp. IB-9374 to belong to GH8 family [55].

Xylose induced cellobiohydrolase activity during cultivation of *Bosea* sp. FBZP-16. The utilization of cellulose and hemicellulose derived monomers is also related to the ability of the strain to perform cellulose and hemicellulose decomposition, as demonstrated by Schuerg et al. [62] for the induction of cellulases with xylose. However, abundant, cost-efficient, and renewable carbon source are prioritized in industry. Although *Bosea* sp. has proven to produce cellulases and xylanases in the presence of simple and defined carbon sources, such as glucose and xylose, these sources are suitable only for enzyme characterization in the lab scale but are too expensive to be used in large scale for production of enzymes. However, as several biomass pretreatments have been developed, the resulting simple sugars can be directly explored to provide a stock of the inducer's monomeric sugars [9].

The presence of different nitrogen sources is beneficial for maximum production of the different (hemi)cellulolytic enzymes in *Bosea* sp. FBZP-16. Indeed, the absence of nitrogen inhibits decomposition of cellulose [32]. Furthermore, malt extract as nitrogen source was efficient in increasing cellobiohydrolase activity. Malt extract is rich in plant based nutrients that has been shown to be involved in

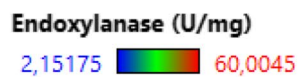
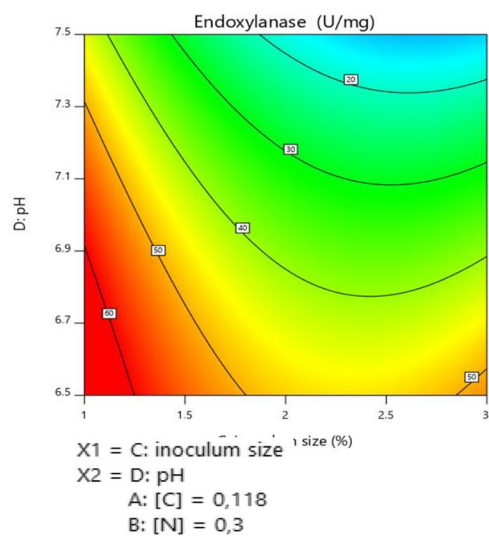
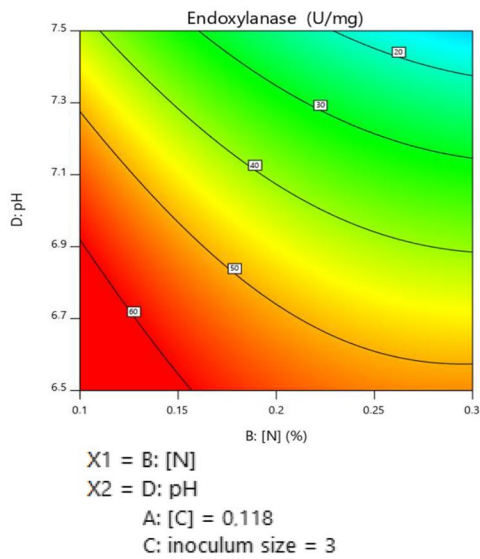
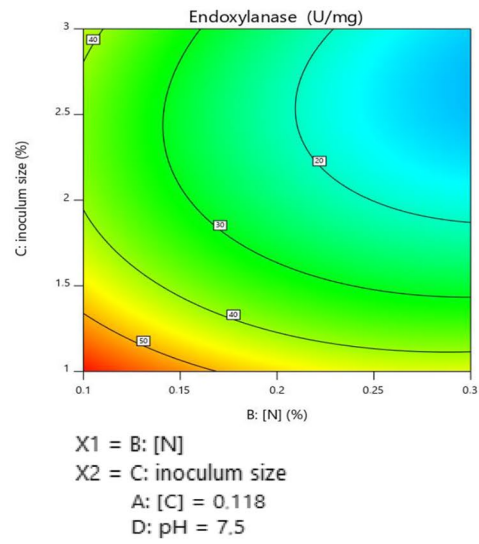
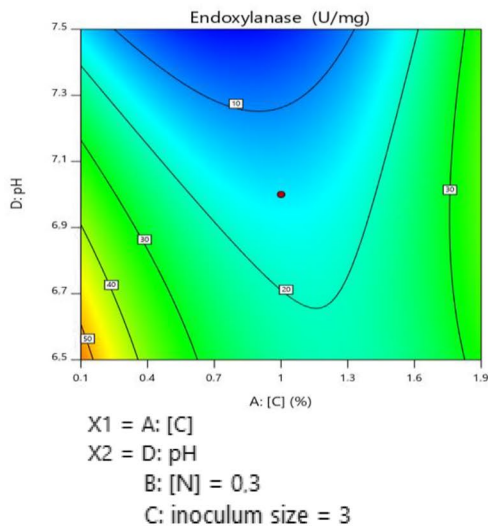
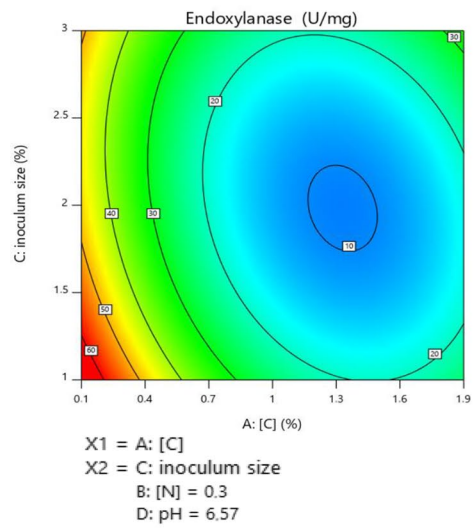
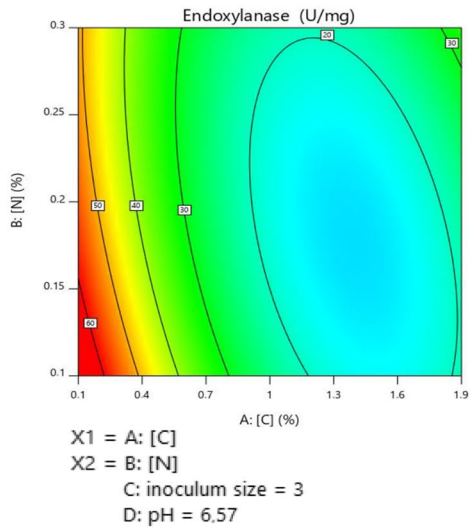


Fig. 3 Contour plots of endoxylanase production from *Bosea* sp. FBZP-16, showing interactions between carbon source concentration, nitrogen source concentration, inoculum size, and pH

enhancing cellulosic and hemicellulosic enzyme production in bacteria [43].

In the context of temperature optimization, *Bosea* sp. FBZP-16 does not withstand high temperatures and would be industrially interesting, if the fermentation is carried out at average temperatures between 30 and 35 °C. Although thermophiles are preferred because of their resistance to harsh pretreatment processes, the fermentations most commonly used on industrial scales occur at temperatures ranging from 30 to 35 °C (for instance *Trichoderma reesei* and *Aspergillus niger*) [16]. Industrial facilities that use mesophilic microorganisms are less expensive than those using thermophilic microorganisms [22]. In addition, mesophilic cellulolytic bacteria can also be directly associated with mesophilic organisms such as *Zymomonas mobilis* or *Saccharomyces cerevisiae*, which are the most successful bio-fuel producers.

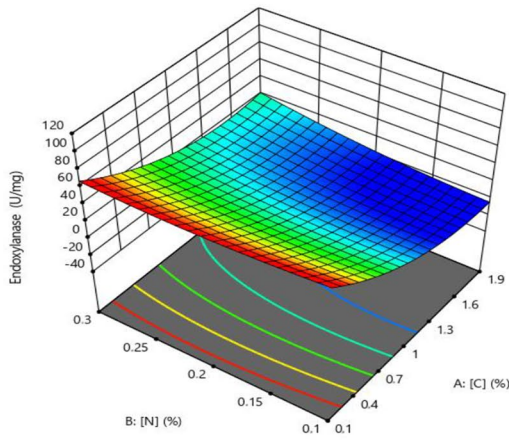
For the investigated microorganism, the shaking frequency of 150 to 300 rpm seems optimal in the investigated range having the best impact on enzyme adsorption/desorption on the (hemi)cellulosic substrate and thus highest monomeric sugar yield [76].

By applying RSM, the quadratic model had a predicted R^2 value of 0.8544 and 0.8781 for cellobiohydrolase and endoxylanase, respectively, confirming the effectiveness of the model, i.e., 85.44% and 87.81% of the total variation in the observed results were attributed to the independent variables. Since the R^2 value is greater than 0.75, the models explain most of the test result's variability [72] and the adjusted R^2 values of 0.684 and 0.736 respectively for cellobiohydrolase and endoxylanase validate the proposed models. Indeed, the R^2 values obtained in these regression models indicate good agreement between predicted and actual cellobiohydrolase and endoxylanase activities. The appropriateness of the obtained regression models is shown in Fig. S-12b and Fig. 5b for cellobiohydrolase and endoxylanase, respectively. The Adeq precision compares the range of predicted values at the design points to the average prediction error. Adeq precision > 4 represents an adequate signal that fit for the studied model [6]. The Adeq precision ratio of 10.44 and 8.99 for cellobiohydrolase and endoxylanase, respectively, indicates that the models are reliable and reproducible in agreement with previous studies [19, 40].

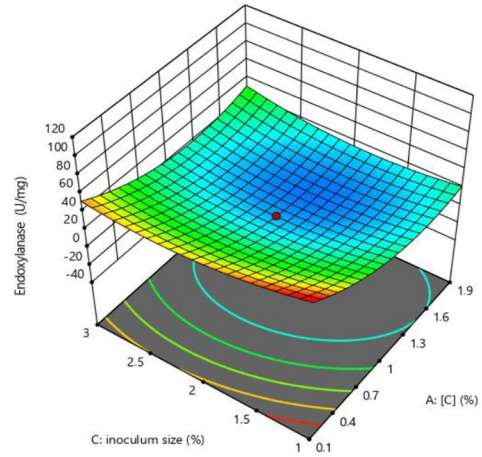
The composition of the medium used in online monitored shake flasks reflects environmental conditions with a high C:N ratio when cellulose and hemicellulose are the major substrates and lower amounts of simple carbon sources are present. α -cellulose was used as reference, being closest to plant-derived cellulose, which is mostly in crystalline

form and recalcitrant to hydrolysis [31]. α -cellulose was demonstrated previously to be a good representative of the alkaline-pretreated biomass used in biorefineries [57]. For sufficient oxygen supply and to insure maximum increase in OTR, the filling volume of RAMOS flask was decreased to 30 mL [39, 73]. Higher volume (40 mL) was used in normal flasks for convenience where evaporation is more likely to occur with cotton plugs. Recently, the use of RAMOS has yielded promising results for the evaluation of cellulose degradation by a strain of *Trichoderma reesei*, using a culture medium with cellulose as a carbon source, providing an effective means for monitoring the growth of cellulose-degrading microorganisms [4]. From RAMOS experiment, it was also demonstrated that the degradation of cellulose can only be enhanced with optimized conditions after the modification of cultivation parameters also reflecting preferential degradation of hemicellulose by *Bosea* sp. FBZP-16. Hemicellulose is easier decomposed than cellulose due to its heterogeneity and amorphous composition that confer random and non-ordered structure. Bacterial cellulases can also be weak as some species lose the capacity to breakdown crystalline cellulose [56]. Any variations limiting cellulose microaccessibility including transport of cellulases and time exposure to the surface of α -cellulose could also affect cellulose hydrolysis [38]. Furthermore, enzymatic hydrolysis do not always occur following binding to cellulose with low interactions [58].

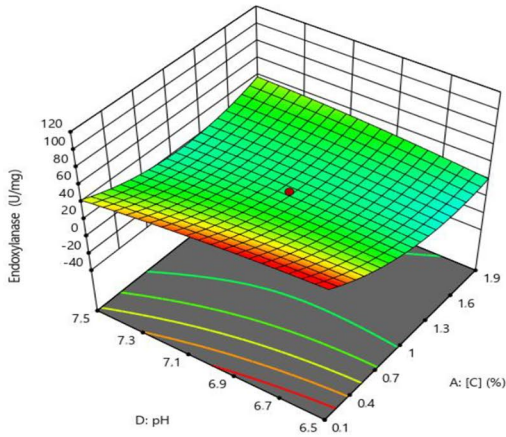
The two-step degradation of xylan results in two peaks between 42 and 54 h culture time of the OTR curve. Later, the decrease of OTR might be explained by enzyme limitation or the substrate no longer being as much accessible as at the beginning. A small peak appearing at about 9 h (Fig. S-13a) might be due to the consumption of yeast extract compounds (2 g/L) used as nitrogen source. No OTR was detected on α -cellulose which correlates with the results from SDS-PAGE and HPAEC-PAD. A band with the same molecular weight (~ 70 kDa) appeared on cellobiose, OrganoCat cellulose, cellulose Sigmacell 20, and RAMOS crude supernatants suggests a β -glucosidase, especially because the band was with higher staining intensity on cellobiose [41, 42]. However, when the bacterium was grown on normal shake flasks (30 °C, 200 rpm, and 40 mL filling volume), the activity of cellobiohydrolases (that targets crystalline cellulose) was significantly higher on Sigmacell 101 cellulose (amorphous) and α -cellulose (less crystalline than Avicel, Sigmacell 20 cellulose, and Sigmacell 50 cellulose). In this case, xylan is still easily hydrolyzed in both RAMOS and normal shake flask cultivations, but the cellulose hydrolysis needs to be further examined until possible detection of rate-limiting factors in OTR. As a result, for a different alternative fermentation configuration, further optimization may be required to initiate growth on cellulose. Indeed, xylanases of bacterial origin are typically released



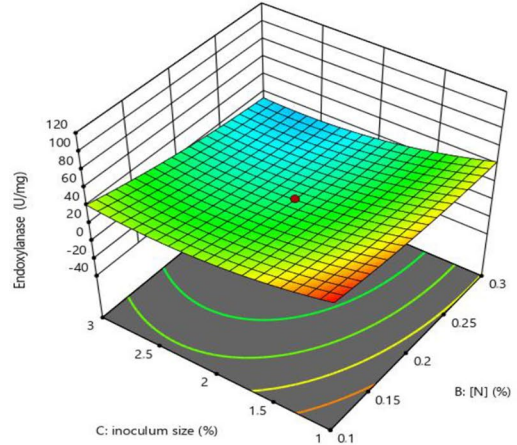
X1 = A: [C]
 X2 = B: [N]
 C: inoculum size = 1
 D: pH = 6.5



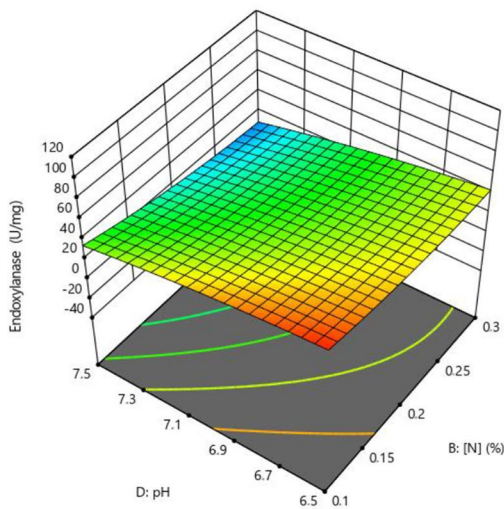
X1 = A: [C]
 X2 = C: inoculum size
 B: [N] = 0.3
 D: pH = 6.5



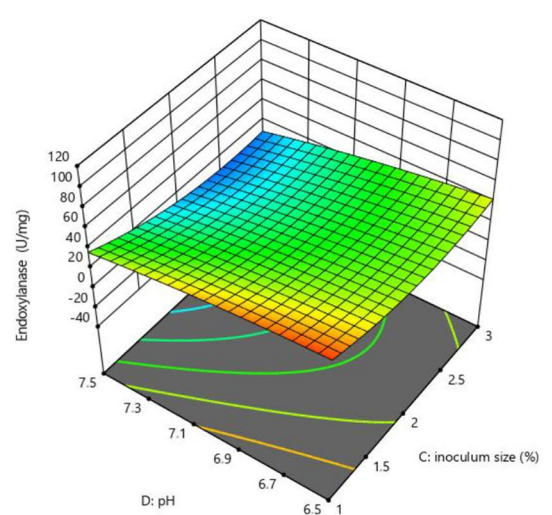
X1 = A: [C]
 X2 = D: pH
 B: [N] = 0.3
 C: inoculum size = 1



X1 = B: [N]
 X2 = C: inoculum size
 A: [C] = 0.1
 D: pH = 7.5



X1 = B: [N]
 X2 = D: pH
 A: [C] = 0.262
 C: inoculum size = 3



X1 = C: inoculum size
 X2 = D: pH
 A: [C] = 0.262
 B: [N] = 0.3

Endoxylanase (U/mg)
 ● Design points above predicted value
 ○ Design points below predicted value
 2.15175 60.0045

◀**Fig. 4** Response surface curves of endoxylanase production

alone in contrast to fungal xylanases that are produced all together with cellulase.

In conclusion, *Bosea* sp. FBZP-16 grew well on soluble and insoluble polysaccharide substrates and effectively hydrolyzed cellulose whether free insoluble cellulose particles or cellulose embedded within other cell wall polymers of raw and/or pretreated lignocellulosic materials. Sophisticated enzyme assays were relevant in this study. Depending on the substrate (cellulosic or hemicellulosic), several proteins with activities can be isolated from *Bosea* sp. FBZP-16. Among the tested lignocellulosic substrates, cellobiohydrolase activity was significantly higher on Sigmacell 101 cellulose and newspaper.

Beechwood xylan revealed the best activities of β -xylosidases as well as higher release of xylose. Regarding the tested nitrogen sources, the highest cellobiohydrolase activities were observed with malt extract. Most enzymes showed the highest activity between 30 and 35 °C. The highest activities of (hemi)cellulolytic enzymes were observed from 150 to 300 rpm with highest yields of glucose and xylose at 150 rpm. This difference in glucose yield might be explained by inadequate mixing when the shaking speed is inferior to 150 rpm and enzyme deactivation due to higher shearing force [61]. However, another study reported better cellulose conversions without shaking than with a shaking speed at 150 rpm [14]. The maximum production of these enzymes was reached from the 3rd to the 9th day of incubation period. This enzymatic profile produced by *Bosea* sp. FBZP-16 during growth showed the potential of different parameters that are promising to reproduce for scale-up fermentation conditions and enzyme purification for further characterization. In this study, OFAT approach was considered for the determination of optimal enzymatic hydrolysis occurring for each physical and qualitative parameter separately. By using statistical methodologies, the fermentation was optimized and resulted in the production of maximum activity of 2796.56 U/mg for cellobiohydrolase and 57.45 U/mg of endoxylanase. In the studied model, the optimum conditions for both cellobiohydrolase and endoxylanase production were successfully and simultaneously identified using the same quadratic model. Confirmatory tests are needed to confirm the validity of the model under the tested medium composition and by varying its components. In this paper, we identified a promising bacterial enzyme producer through the combination of different statistical optimization approaches while varying culture growth conditions to understand enzyme production. The best conditions to obtain a suitable mixture of enzymes would be explored to design enzyme cocktails in the context of a biotechnological application. For future experiments when conceptualizing and

designing enzyme applications, it is important to conduct a saccharification experiment which employs an enzyme preparation obtained under optimal conditions. Aspects of enzymatic degradation can also be considered according to the amount of released monomeric sugars for saccharification technologies needed on the commercial scale. The commercial production of cellulosic ethanol is facing challenges of high production costs involved in microbial bioreactors and lignocellulosic pretreatment for cellulases [15]. Furthermore, commercial enzyme cocktails continue to be a bottleneck in hydrolysis due to their costs [28]. The cost of transporting enzymes from a central facility to a biorefinery can make a significant difference for local biorefineries [27]. Hence, using the in-house produced enzymes would be more cost-effective than using commercially available cellulases or hemicellulases.

Supplementary Information The online version contains supplementary material available at <https://doi.org/10.1007/s13399-021-02044-1>.

Acknowledgements The authors acknowledge Anne Lunze (Chair of Enzyme Process Technology, RWTH Aachen University, Aachen, Germany) and Lamia Medouni-Haroune (Laboratoire de Microbiologie Appliquée, Université de Bejaia) for providing cup plant and olive pomace, respectively.

Author contribution AAH conducted the wet laboratory experiments, wrote the manuscript, designed the visualization, and performed the statistical analysis. AAH, NA, and SB designed the study. JL, BH, and JB contributed to the data analysis acquired from the RAMOS device. NA, SB, and JB supervised the study, lead the project, provided resources, and supported in acquiring funding. ZA and AB participated in the validation of the RSM data analysis. All the authors read the manuscript prior to submission, contributed to the writing-review, and editing of the manuscript.

Funding This work was supported by the Algerian Ministry of Higher Education and Scientific Research, by granting a scholarship in the framework of Programme National Exceptionnel (PNE) in respect of the academic year 2016–2017. This work was also supported by Aachener Verfahrenstechnik (AVT) of RWTH Aachen University. Part of this work was performed as part of the Cluster of Excellence “Tailor-Made Fuels from Biomass,” which is funded by the Excellence Initiative of the German federal and state government to promote science and research at German universities.

Data availability All data and information generated during this study are available.

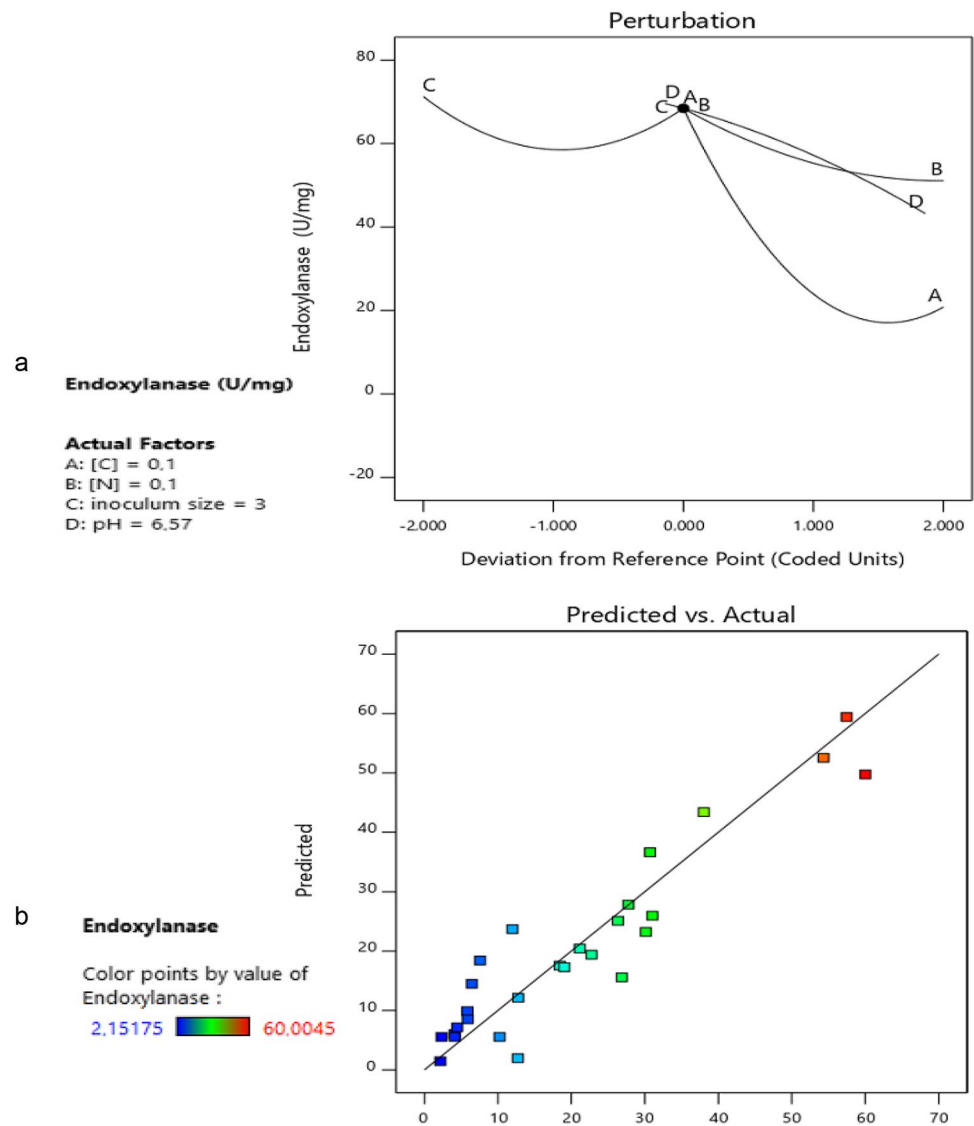
Ethical statement.

This article does not contain any studies with human participants or animals performed by any of the authors.

Declarations

Competing interests The authors declare no competing interests.

Fig. 5 Perturbation graphs and parity plot representing the distribution of actual vs. predicted values of endoxylanase (**a**, **b**)



References

- Anderlei T, Büchs J (2001) Device for sterile online measurement of the oxygen transfer rate in shaking flasks. *Biochem Eng J* 7:157–162. [https://doi.org/10.1016/S1369-703X\(00\)00116-9](https://doi.org/10.1016/S1369-703X(00)00116-9)
- Anderlei T, Zang W, Papaspyrou M, Büchs J (2004) Online respiration activity measurement (OTR, CTR, RQ) in shake flasks. *Biochem Eng J* 17:187–194. [https://doi.org/10.1016/S1369-703X\(03\)00181-5](https://doi.org/10.1016/S1369-703X(03)00181-5)
- Anders N, Humann H, Langhans B, Spiess AC (2015) Simultaneous determination of acid-soluble biomass-derived compounds using high performance anion exchange chromatography coupled with pulsed amperometric detection. *Anal Methods* 7:7866–7873. <https://doi.org/10.1039/c5ay01371b>
- Antonov E, Wirth S, Gerlach T, Schlembach I, Rosenbaum MA, Regestein L (2016) Efficient evaluation of cellulose digestibility by *Trichoderma reesei* Rut-C30 cultures in online monitored shake flasks. *Microb Cell Fact* 1–17 <https://doi.org/10.1186/s12934-016-0567-7>
- Azzouz Z, Bettache A, Boucherba N, Amghar Z, Benallaoua S (2020) Optimization of xylanase production by newly isolated strain *Trichoderma afroharzianum* isolate AZ 12 in solid state fermentation using response surface methodology. *Cellulose Chem Technol* 54:451–462. <https://doi.org/10.35812/CelluloseChemTechnol.2020.54.46>
- Azzouz Z, Bettache A, Djinni I, Boucherba N, Benallaoua S (2020b) Biotechnological production and statistical optimization of fungal xylanase by bioconversion of the lignocellulosic biomass residues in solid-state fermentation. *Biomass Convers Biorefinery* 1–13 <https://doi.org/10.1007/s13399-020-01018-z>
- Bachir bey M, Meziat L, Benchikh Y, Louaileche H (2014) Deployment of response surface methodology to optimize recovery of dark fresh fig (*Ficus carica* L., var. Azenjar) total phenolic compounds and antioxidant activity. *Food Chem* 162:277–282. <https://doi.org/10.1016/J.FOODCHEM.2014.04.054>
- Baldrian P (2009) Microbial enzyme-catalyzed processes in soils and their analysis. *Plant, Soil Environ* 55:370–378. <https://doi.org/10.1007/s11104-008-9731-0>
- Baruah J, Nath BK, Sharma R, Kumar S, Deka RC, Baruah DC, Kalita E (2018) Recent trends in the pretreatment of

- lignocellulosic biomass for value-added products. *Front. Energy Res.* 6
10. Belhadji L, HadjSadok A, Moulai-Mostefa N (2018) Design and characterization of calcium-free *in-situ* gel formulation based on sodium alginate and chitosan. *Drug Dev Ind Pharm* 44:662–669. <https://doi.org/10.1080/03639045.2017.1408640>
 11. Benmeziane A, Boulekbache-Makhlouf L, Mapelli-Brahm P, Khaled Khodja N, Remini H, Madani K, Meléndez-Martínez AJ (2018) Extraction of carotenoids from cantaloupe waste and determination of its mineral composition. *Food Res Int* 111:391–398. <https://doi.org/10.1016/J.FOODRES.2018.05.044>
 12. Berlin A (2013) No barriers to cellulose breakdown. *Science* 342:1454–1456. <https://doi.org/10.1126/science.1247697>
 13. Bettache A, Abdelaziz M, Estelle C, Mouloud K, Nawel B, Nabila B, Francis D, Said B (2013) Optimization and partial characterization of endoglucanase produced by streptomyces SP. B-PNG23. *Arch Biol Sci* 65:549–558. <https://doi.org/10.2298/ABS1302549A>
 14. Bhagia S, Dhir R, Kumar R, Wyman CE (2018) Deactivation of cellulase at the air-liquid interface is the main cause of incomplete cellulose conversion at low enzyme loadings. *Sci Rep* 8:1–12. <https://doi.org/10.1038/s41598-018-19848-3>
 15. Bisen PS, Debnath M, Prasad GBKS (2012) Microbes: concepts and applications. 699
 16. Biswas R, Persad A, Bisaria VS (2014) Production of cellulolytic enzymes. Bioprocessing of renewable resources to commodity bioproducts. John Wiley & Sons Inc, Hoboken, NJ, USA, pp 105–132
 17. Boucherba N, Benallaoua S, Copinet E, Hebal H, Duchiron F (2011) Production and partial characterization of xylanase produced by *Jonesia denitrificans* isolated in Algerian soil. *Process Biochem* 46:519–525. <https://doi.org/10.1016/j.procbio.2010.10.003>
 18. Bouiche C, Boucherba N, Benallaoua S, Martinez J, Diaz P, Pastor FIJ, Valenzuela SV (2020) Differential antioxidant activity of glucuronoxyloligosaccharides (UXOS) and arabinoxyloligosaccharides (AXOS) produced by two novel xylanases. *Int J Biol Macromol* 155:1075–1083. <https://doi.org/10.1016/j.ijbmac.2019.11.073>
 19. Chen W, Wang WP, Zhang HS, Huang Q (2012) Optimization of ultrasonic-assisted extraction of water-soluble polysaccharides from *Boletus edulis* mycelia using response surface methodology. *Carbohydr Polym* 87:614–619. <https://doi.org/10.1016/J.CARBPOL.2011.08.029>
 20. Copete-Pertuz LS, Alandete-Novoa F, Plácido J, Correa-Londoño GA, Mora-Martínez AL (2019) Enhancement of ligninolytic enzymes production and decolourising activity in *Leptosphaerulina* sp. by co-cultivation with *Trichoderma viride* and *Aspergillus terreus*. *Sci Total Environ* 646:1536–1545. <https://doi.org/10.1016/J.SCITOTENV.2018.07.387>
 21. Cürten C, Anders N, Juchem N, Ihling N, Volkenborn K, Knapp A, Jaeger K-E, Büchs J, Spiess AC (2018) Fast automated online xylanase activity assay using HPAEC-PAD. *Anal Bioanal Chem* 410:57–69. <https://doi.org/10.1007/s00216-017-0712-0>
 22. Damhus T, Kaasgaard S, Olsen H (2013) *Enzymes at work*, 4th edn.
 23. Djinni I, Djoudi W, Souagui S, Rabia F, Rahmouni S, Mancini I, Kecha M (2018) *Streptomyces thermoviolaceus* SRC3 strain as a novel source of the antibiotic adjuvant streptazolin: a statistical approach toward the optimized production. *J Microbiol Methods* 148:161–168. <https://doi.org/10.1016/J.MIMET.2018.04.008>
 24. Dondelinger E, Aubry N, Ben Chaabane F, Cohen C, Tayeb J, Rémond C (2016) Contrasted enzymatic cocktails reveal the importance of cellulases and hemicellulases activity ratios for the hydrolysis of cellulose in presence of xylans. *AMB Express*. <https://doi.org/10.1186/s13568-016-0196-x>
 25. Dutta SK, Chakraborty S (2016) Pore-scale dynamics of enzyme adsorption, swelling and reactive dissolution determine sugar yield in hemicellulose hydrolysis for biofuel production. *Sci Rep* 6:38173. <https://doi.org/10.1038/srep38173>
 26. Edehech A, Zied Z, Aloui F, Smichi N, Noiriell A, Abousalham A, Gargouri Y (2019) Production, purification and biochemical characterization of a thermoactive, alkaline lipase from a newly isolated *Serratia* sp. W3 Tunisian strain. *Int J Biol Macromol* 123:792–800. <https://doi.org/10.1016/J.IJBIOMAC.2018.11.050>
 27. Ellilä S, Fonseca L, Uchima C, Cota J, Goldman GH, Saloheimo M, Sacon V (2017) Siika-aho M (2017) Development of a low-cost cellulase production process using *Trichoderma reesei* for Brazilian biorefineries. *Biotechnol Biofuels* 10(10):1–17. <https://doi.org/10.1186/S13068-017-0717-0>
 28. Ferreira R da G, Azzoni AR, Freitas S (2018) Techno-economic analysis of the industrial production of a low-cost enzyme using *E. coli*: the case of recombinant β -glucosidase. *Biotechnol Biofuels* 2018 111 11:1–13. <https://doi.org/10.1186/S13068-018-1077-0>
 29. Garcia Medeiros R, Hanada R, Filho EXF (2003) Production of xylan-degrading enzymes from Amazon forest fungal species. *Int Biodeterior Biodegrad* 52:97–100. [https://doi.org/10.1016/S0964-8305\(02\)00179-8](https://doi.org/10.1016/S0964-8305(02)00179-8)
 30. Grande PM, Viell J, Theysen N, Marquardt W, Domínguez de María P, Leitner W (2015) Fractionation of lignocellulosic biomass using the OrganoCat process. *Green Chem* 17:3533–3539. <https://doi.org/10.1039/C4GC02534B>
 31. Hiras J, Wu YW, Deng K, Nicora CD, Aldrich JT, Frey D, Kolinko S, Robinson EW, Jacobs JM, Adams PD, Northen TR, Simmons BA, Singer SW (2016) Comparative community proteomics demonstrates the unexpected importance of actinobacterial glycoside hydrolase family 12 protein for crystalline cellulose hydrolysis. *MBio* 7:1–9. <https://doi.org/10.1128/mBio.01106-16>
 32. Honey Thet Paing Htway 1 San San Yu, 1 2 Zaw Ko Latt, 2Khin Pyone Yi1 (2018) Improvement of cellulolytic activity in cellulolytic nitrogen-fixing bacteria by transposon mutagenesis. *J Bacteriol Microb Open Access* 6:1–7. <https://doi.org/10.15406/JBMOA.2018.06.00193>
 33. Houfani AA, Anders N, Spiess AC, Baldrian P, Benallaoua S (2019) Trends in the analysis of enzymatic degradation of cellulose and hemicellulose – a review. *Biomass and Bioenergy*
 34. Houfani AA, Anders N, Spiess AC, Baldrian P, Benallaoua S (2020) Insights from enzymatic degradation of cellulose and hemicellulose to fermentable sugars—a review. *Biomass and Bioenergy* 134:105481
 35. Houfani AA, Větrovský T, Baldrian P, Benallaoua S (2017) Efficient screening of potential cellulases and hemicellulases produced by *Bosea* sp. FBZP-16 using the combination of enzyme assays and genome analysis. *World J Microbiol Biotechnol* 33:1–14. <https://doi.org/10.1007/s11274-016-2198-x>
 36. Ihling N, Bittner N, Diederichs S, Schelden M, Korona A, Höfler GT, Fulton A, Jaeger K-E, Honda K, Ohtake H, Büchs J (2018) Online measurement of the respiratory activity in shake flasks enables the identification of cultivation phases and patterns indicating recombinant protein production in various *Escherichia coli* host strains. *Biotechnol Prog*. <https://doi.org/10.1002/btpr.2600>
 37. Jäger G, Wu Z, Garschhammer K, Engel P, Klement T, Rinaldi R, Spiess A, Büchs J (2010) Practical screening of purified cellobiohydrolases and endoglucanases with alpha-cellulose and specification of hydrodynamics. *Biotechnol Biofuels* 3:18. <https://doi.org/10.1186/1754-6834-3-18>
 38. Kafle K, Shin H, Lee CM, Park S, Kim SH (2015) Progressive structural changes of Avicel, bleached softwood, and bacterial cellulose during enzymatic hydrolysis. *Sci Rep* 5. <https://doi.org/10.1038/srep15102>

39. Kensy F, Engelbrecht C, Büchs J (2009) Scale-up from microtiter plate to laboratory fermenter: evaluation by online monitoring techniques of growth and protein expression in *Escherichia coli* and *Hansenula polymorpha* fermentations. *Microb Cell Fact* 8:68. <https://doi.org/10.1186/1475-2859-8-68>
40. Khusro A, Kaliyan BK, Al-Dhabi NA, Arasu MV, Agastian P (2016) Statistical optimization of thermo-alkali stable xylanase production from *Bacillus tequilensis* strain ARMATI. *Electron J Biotechnol* 22:16–25. <https://doi.org/10.1016/J.EJBT.2016.04.002>
41. Kim KH, Brown KM, Harris PV, Langston JA, Cherry JR (2007) A proteomics strategy to discover β -glucosidases from *Aspergillus fumigatus* with two-dimensional page in-gel activity assay and tandem mass spectrometry. *J Proteome Res* 6:4749–4757. <https://doi.org/10.1021/pr070355i>
42. Korotkova OG, Semenova MV, Morozova VV, Zorov IN, Sokolova LM, Bubnova TM, Okunev ON, Sinitsyn AP (2009) Isolation and properties of fungal β -glucosidases. *Biochem* 74:569–577. <https://doi.org/10.1134/S0006297909050137>
43. Lasa AV, Mašínová T, Baldrian P, Fernández-López M (2019) Bacteria from the endosphere and rhizosphere of *Quercus* spp. Use mainly cell wall-associated enzymes to decompose organic matter. *PLoS One* 14:e0214422. <https://doi.org/10.1371/journal.pone.0214422>
44. Lee CC, Smith M, Kibblewhite-Accinelli RE, Williams TG, Wagschal K, Robertson GH, Wong DWS (2006) Isolation and characterization of a cold-active xylanase enzyme from *Flavobacterium* sp. *Curr Microbiol* 52:112–116. <https://doi.org/10.1007/s00284-005-4583-9>
45. Lever M (1973) Colorimetric and fluorometric carbohydrate determination with p-hydroxybenzoic acid hydrazide. *Biochem Med* 7:274–281. [https://doi.org/10.1016/0006-2944\(73\)90083-5](https://doi.org/10.1016/0006-2944(73)90083-5)
46. Liao JC, Mi L, Pontrelli S, Luo S (2016) Fuelling the future: microbial engineering for the production of sustainable biofuels. *Nat Rev Microbiol* 14:288–304
47. Ling HH (2016) Batch submerged fermentation in shake flask culture and bioreactor: influence of different agricultural residuals as the substrate on the optimization of xylanase production by *Bacillus subtilis* and *Aspergillus brasiliensis*. *J Appl Biotechnol Bioeng* 1:1–9. <https://doi.org/10.15406/jabb.2016.01.00016>
48. Lunze A, Heyman B, Chammakhi Y, Eichhorn M, Büchs J, Anders N, Spiess AC (2020) Investigation of *Silphium perfoliatum* as feedstock for a liquid hot water-based biorefinery process towards 2,3-butanediol. *Bioenergy Res* 1–16. <https://doi.org/10.1007/s12155-020-10194-9>
49. Mäki-Arvela P, Salmi T, Holmbom B, Willför S, Murzin DY (2011) Synthesis of sugars by hydrolysis of hemicelluloses—a review. *Chem Rev* 111:5638–5666. <https://doi.org/10.1021/cr2000042>
50. Mechri S, Kriaa M, Ben Elhouel Berrouina M, Omrane Benmradi M, Zeraï Jaouadi N, Rekik H, Bouacem K, Bouanane-Darenfed A, Chebbi A, Sayadi S, Chamkha M, Bejar S, Jaouadi B (2017) Optimized production and characterization of a detergent-stable protease from *Lysinibacillus fusiformis* C250R. *Int J Biol Macromol* 101:383–397. <https://doi.org/10.1016/J.IJBIOMAC.2017.03.051>
51. Medouni-Adrar S, Boulekbache-Makhlouf L, Cadot Y, Medouni-Haroune L, Dahmoune F, Makhoukhe A, Madani K (2015) Optimization of the recovery of phenolic compounds from Algerian grape by-products. *Ind Crops Prod* 77:123–132. <https://doi.org/10.1016/j.indcrop.2015.08.039>
52. Medouni-Haroune L, Zaidi F, Roussos S, Desseaux V, Medouni-Adrar S, Kecha M (2017) Solid state fermentation based olive pomace using streptomyces strains: a preliminary study. *Asian J Biotechnol Bioresour Technol* 2:1–9. <https://doi.org/10.9734/AJB2T/2017/36548>
53. Messis A, Bettache A, Brahami A, Kecha M, Benallaoua S (2014) Optimization of antifungal production from a novel strain *Streptomyces* sp. TKJ2 using response surface methodology. *Med Chem Res* 23:310–316. <https://doi.org/10.1007/s00044-013-0627-z>
54. Murugan S, Arnold D, Pongiya UD, Narayanan PM (2011) Production of xylanase from *arthrobacter* sp. MTCC 6915 using saw dust as substrate under solid state fermentation. *Enzyme Res* 2011. <https://doi.org/10.4061/2011/696942>
55. Ogura J, Toyoda A, Kurosawa T, Chong AL, Chohnan S, Masaki T (2006) Purification, characterization, and gene analysis of cellulase (Cel8A) from *Lysobacter* sp. IB-9374. *Biosci Biotechnol Biochem* 70:2420–2428. <https://doi.org/10.1271/bbb.60157>
56. Peng X, Qiao W, Mi S, Jia X, Su H, Han Y (2015) Characterization of hemicellulase and cellulase from the extremely thermophilic bacterium *Caldicellulosiruptor owensensis* and their potential application for bioconversion of lignocellulosic biomass without pretreatment. *Biotechnol Biofuels*. <https://doi.org/10.1186/s13068-015-0313-0>
57. Percival Zhang YH, Himmel ME, Mielenz JR (2006) Outlook for cellulase improvement: screening and selection strategies. *Biotechnol Adv* 24:452–481. <https://doi.org/10.1016/j.biotechadv.2006.03.003>
58. Pihlajaniemi V, Sipponen MH, Kallioinen A, Nyyssölä A, Laakso S (2016) Rate-constraining changes in surface properties, porosity and hydrolysis kinetics of lignocellulose in the course of enzymatic saccharification. *Biotechnol Biofuels* 9. <https://doi.org/10.1186/s13068-016-0431-3>
59. Rahman MS, Fernando S, Ross B, Wu J, Qin W (2018) Endoglucanase (EG) activity assays. *Methods Mol Biol* 1796:169–183. https://doi.org/10.1007/978-1-4939-7877-9_13
60. Rakotoarivonina H, Hermant B, Aubry N, Rabenoelina F, Baillicul F, Rémond C (2014) Dynamic study of how the bacterial breakdown of plant cell walls allows the reconstitution of efficient hemicellulase cocktails. *Bioresour Technol* 170:331–341. <https://doi.org/10.1016/j.biortech.2014.07.097>
61. Robak K, Balcerek M (2020) Current state-of-the-art in ethanol production from lignocellulosic feedstocks. *Microbiol Res* 240:126534
62. Schuerg T, Prah J-P, Gabriel R, Harth S, Tachea F, Chen C-S, Miller M, Masson F, He Q, Brown S, Mirshiahi M, Liang L, Tom LM, Tanjore D, Sun N, Pray TR, Singer SW (2017) Xylose induces cellulase production in *Thermoascus aurantiacus*. *Biotechnol Biofuels* 10:271. <https://doi.org/10.1186/s13068-017-0965-z>
63. Sharma D, Garlapati VK, Goel G (2016) Bioprocessing of wheat bran for the production of lignocellulolytic enzyme cocktail by *Cotyledia pannosa* under submerged conditions. *Bioengineered* 7:88–97. <https://doi.org/10.1080/21655979.2016.1160190>
64. Singhanian RR, Patel AK, Sukumaran RK, Larroche C, Pandey A (2013) Role and significance of beta-glucosidases in the hydrolysis of cellulose for bioethanol production. *Bioresour Technol* 127:500–507. <https://doi.org/10.1016/J.BIORTECH.2012.09.012>
65. Souagui-Boudries S, Warda D, Hafid B, Mas B, Valerie L (2018) Characterization and statistical optimization of culture medium for improving production of antifungal compounds by *Streptomyces albidoflavus* S19 isolated from wastewater. *Anti-Infective Agents* 16. <https://doi.org/10.2174/2211352516666180813102424>
66. Souagui Y, Tritsch D, Grosdemange-Billiard C, Kecha M (2015) Optimization of antifungal production by an alkaliphilic and halotolerant actinomycete, *Streptomyces* sp. SY-BS5, using response surface methodology. *J Mycol Med* 25:108–115. <https://doi.org/10.1016/J.MYCMED.2014.12.004>
67. Tabssum F, Irfan M, Shakir HA, Qazi JI (2018) RSM based optimization of nutritional conditions for cellulase mediated

- Saccharification by *Bacillus cereus*. *J Biol Eng* 12:7. <https://doi.org/10.1186/s13036-018-0097-4>
68. Tan H, Miao R, Liu T, Yang L, Yang Y, Chen C, Lei J, Li Y, He J, Sun Q, Peng W, Gan B, Huang Z (2018) A bifunctional cellulase-xylanase of a new *Chryseobacterium* strain isolated from the dung of a straw-fed cattle. *Microb Biotechnol* 11:381–398. <https://doi.org/10.1111/1751-7915.13034>
69. Thornbury M, Sicheri J, Slaine P, Getz LJ, Finlayson-Trick E, Cook J, Guinard C, Boudreau N, Jakeman D, Rohde J, McCormick C (2019) Characterization of novel lignocellulose-degrading enzymes from the porcupine microbiome using synthetic metagenomics. *PLoS One* 14 <https://doi.org/10.1371/journal.pone.0209221>
70. vom Stein T, Grande PM, Kayser H, Sibilla F, Leitner W, Domínguez de María P (2011) From biomass to feedstock: one-step fractionation of lignocellulose components by the selective organic acid-catalyzed depolymerization of hemicellulose in a biphasic system. *Green Chem* 13:1772. <https://doi.org/10.1039/c1gc00002k>
71. Walker JA, Takasuka TE, Deng K, Bianchetti CM, Udell HS, Prom BM, Kim H, Adams PD, Northen TR, Fox BG (2015) Multifunctional cellulase catalysis targeted by fusion to different carbohydrate-binding modules. *Biotechnol Biofuels* 8:220. <https://doi.org/10.1186/s13068-015-0402-0>
72. Wan Omar WNN, Nordin N, Mohamed M, Amin NAS (2009) A two-step biodiesel production from waste cooking oil: optimization of pre-treatment step. *J Appl Sci* 9:3098–3103. <https://doi.org/10.3923/JAS.2009.3098.3103>
73. Wewetzer SJ, Kunze M, Ladner T, Luchterhand B, Roth S, Rahman N, Kloß R, Costa E, Silva A, Regestein L, Büchs J (2015) Parallel use of shake flask and microtiter plate online measuring devices (RAMOS and BioLector) reduces the number of experiments in laboratory-scale stirred tank bioreactors. *J Biol Eng* 9:9. <https://doi.org/10.1186/s13036-015-0005-0>
74. Willis JD, Oppert C, Jurat-Fuentes JL (2010) Methods for discovery and characterization of cellulolytic enzymes from insects. *Insect Sci* 17:184–198. <https://doi.org/10.1111/j.1744-7917.2010.01322.x>
75. Yan Q, Miazek K, Grande PM, Domínguez De María P, Leitner W, Modigell M (2014) Mechanical pretreatment in a screw press affecting chemical pulping of lignocellulosic biomass. *Energy Fuels* 28:6981–6987. <https://doi.org/10.1021/ef501706w>
76. Zheng F, Ding S (2013) Processivity and enzymatic mode of a glycoside hydrolase family 5 endoglucanase from *Volvariella volvacea*. *Appl Environ Microbiol* 79:989–996. <https://doi.org/10.1128/AEM.02725-12>

Publisher's Note Springer Nature remains neutral with regard to jurisdictional claims in published maps and institutional affiliations.